

Kinetic dissipation and anisotropic heating in a turbulent collisionless plasma

T. N. Parashar, M. A. Shay, P. A. Cassak, and W. H. Matthaeus

*Department of Physics & Astronomy, 217 Sharp Lab,
University of Delaware, Newark, Delaware 19716, USA*

(Dated: May 28, 2019)

Abstract

The kinetic evolution of the Orszag-Tang vortex is studied using collisionless hybrid simulations. In the magnetohydrodynamic regime this vortex leads rapidly to broadband turbulence. Significant differences from MHD arise at small scales, where the fluid scale energy dissipates into heat almost exclusively through the magnetic field because the protons are decoupled from the magnetic field. Although cyclotron resonance is absent, the protons heat preferentially in the plane perpendicular to the mean field, as in the corona and solar wind. Effective transport coefficients are calculated.

Magnetohydrodynamic (MHD) models are the most tractable plasma dynamical models, yet remain of formidable complexity when turbulence develops. Computations of MHD turbulence generally employ small but nonzero viscosity and/or resistivity, which allows a broad band of dynamical length scales and concentrates dissipation at small scales. However, such models do not address the origin, or even the correct functional representation, of the physical processes responsible for conversion of fluid scale energy irreversibly into kinetic degrees of freedom. We refer to these processes as “dissipation.” Plasma dissipation is of current interest in coronal heating and the acceleration of the solar wind [1], turbulence in the interplanetary medium [2], energy storage and release in the magnetosphere [3], and in a variety of other plasma and astrophysical contexts [4].

In the solar wind [5, 6], observed magnetic spectrum involves three ranges of spatial scale [7] – the energy containing scale (related to system size, external driving, or boundary conditions), an intermediate, often power law inertial range, and a small scale kinetic dissipation range, where fluid energy is converted into kinetic degrees of freedom. Turbulence both in the solar wind (plasma $\beta = (\text{thermal speed}/\text{Alfvén speed})^2 \sim 1$) and in the corona ($\beta \ll 1$) shows substantial proton heating and, notably, preferred heating in the direction perpendicular to the mean magnetic field [1, 6]. This heating might have a variety of sources, including shocks and wave-particle interactions involving non thermal distributions such as pickup ions, but the ubiquity of broadband Kolmogoroff-like fluctuations suggests that kinetic absorption of fluid energy at or beyond the high wavenumber end of the inertial range plays an important role.

Previous attempts to numerically model plasma dissipation, e.g., by employing hyper-resistivity, hyperviscosity or indirectly by including the Hall or finite Larmor radius effects (see [8]), include only selected approximations to kinetic effects, and therefore are not able to explain the wider range of mechanisms available to the kinetic plasma. A fundamental demonstration of the perpendicular heating and dissipation that is observed in a medium such as the solar wind is needed. We attempt this here.

The difficulty in such a demonstration is the requirement of treating a wide range of length scales, which is intrinsically difficult with limited computational resources. As a first step in understanding the intricacies of plasma dissipation, we study kinetic dissipation starting from a well studied MHD initial configuration – the Orszag-Tang vortex [9] – using a hybrid code. The Orszag-Tang initial conditions, in terms of the magnetic field \mathbf{B} and the

velocity field \mathbf{v} , are

$$\mathbf{B} = -\sin y \hat{\mathbf{x}} + \sin 2x \hat{\mathbf{y}}; \quad \mathbf{v} = -\sin y \hat{\mathbf{x}} + \sin x \hat{\mathbf{y}} \quad (1)$$

in normalized units discussed later. This leads immediately to strong nonlinear couplings, producing cascade-like activity that might reasonably approximate the highest wavenumber decade of the inertial range. These couplings, which are dominantly local in wavenumber, in turn drive the dissipation range. Robust production of nonlinear activity is a motivation for frequent use of Orszag-Tang vortex to validate numerical schemes (see e.g. [10]). By choosing a computational domain with approximately one decade of scale in the MHD range and another in the kinetic range, we can study the conversion of strongly driven MHD fluctuations into kinetic motions.

We find that the hybrid simulation results are similar to MHD simulations of the Orszag-Tang vortex at large scales, but display significant differences at small scales where kinetic effects are important. Energy is dissipated into proton heating almost exclusively through the magnetic field, as opposed to bulk flow. The proton heating occurs preferentially in the plane perpendicular to the mean magnetic field. This occurs even though cyclotron resonance effects, often invoked for dissipation in the solar wind [11], are absent in the present 2.5D simulations. Finally, we calculate effective transport coefficients from the hybrid simulations to determine the applicability of constant resistivity η and viscosity ν to collisionless systems, finding that the assumption is potentially reasonable for η , but untenable for ν .

The physics of the Orszag-Tang vortex has been previously studied using incompressible [9] and compressible [12] MHD simulations. An antecedent of the present study compared global behavior of hybrid and Hall MHD simulations [13], but included a mean in-plane magnetic field while not adequately resolving the proton inertial length.

We use the hybrid code P3D [14] in 2.5D, which evolves

$$\frac{d\mathbf{x}_i}{dt} = \mathbf{v}_i; \quad \frac{d\mathbf{v}_i}{dt} = \frac{1}{\epsilon_H} (\mathbf{E}' + \mathbf{v}_i \times \mathbf{B}) \quad (2)$$

$$\frac{\partial \mathbf{B}'}{\partial t} = \nabla \times (\mathbf{v} \times \mathbf{B}) + \epsilon_H \nabla \times \left(\frac{\mathbf{J}}{n} \times \mathbf{B}' \right) \quad (3)$$

$$\mathbf{B}' = \left(1 - \frac{m_e}{m_i} \epsilon_H^2 \nabla^2 \right) \mathbf{B}, \quad \mathbf{E}' = \mathbf{B} \times \left(\mathbf{v} - \epsilon_H \frac{\mathbf{J}}{n} \right) \quad (4)$$

where $\mathbf{J} = \nabla \times \mathbf{B}$ is the current density, $\epsilon_H \equiv c/(L_0 \omega_{pi})$ is the normalized proton inertial length, m_e and m_i are the electron and proton masses, \mathbf{x}_i and \mathbf{v}_i are the positions and

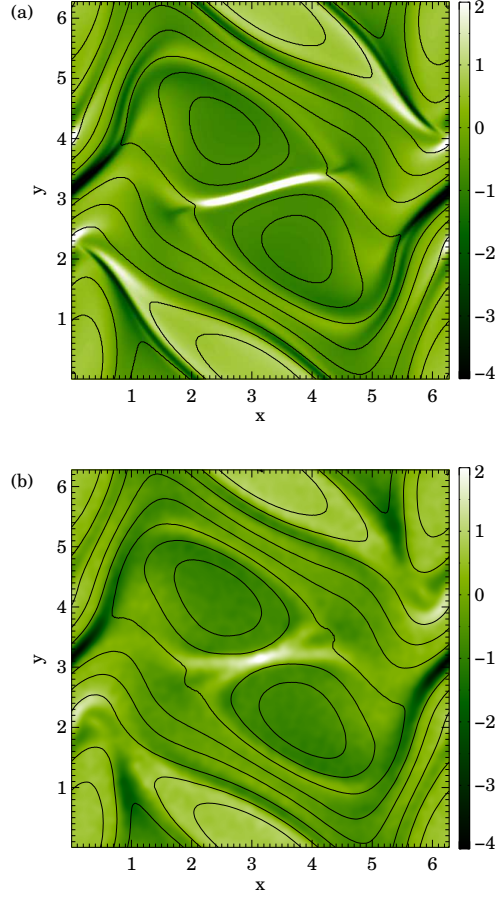


FIG. 1: (Color online) Current density with magnetic flux contours at $t=1.96$ in (a) fluid and (b) hybrid simulations.

velocities of the individual protons, and \mathbf{v} is the bulk flow speed. Length is normalized to L_0 , velocities to $V_0 = B_0/(4\pi mn_0)^{1/2}$, time to $t_0 = L_0/V_0$, and temperature to $B_0^2/(4\pi n_0)$. Average density is n_0 , and B_0 is the root mean square in-plane magnetic field. Magnetic field \mathbf{B} is determined from \mathbf{B}' using the multigrid method [15]. The code assumes quasi-neutrality. The electron temperature is zero and is not updated.

The simulated domain is a square box of side 2π covered by a 512^2 grid. We set $\epsilon_H = 2\pi/25.6$ and $m_e = 0.04m_i$. There are ~ 2.6 million protons loaded with an initial maxwellian distribution having a uniform temperature = 8. No artificial dissipation is present other than grid scale dissipation. An out-of-plane (guide) magnetic field of strength 5 (giving total $\beta = 2nT/B^2 \approx 0.62$) reduces the system compressibility. We further promote incompressibility by imposing an initial constant density n_0 with small perturbations that

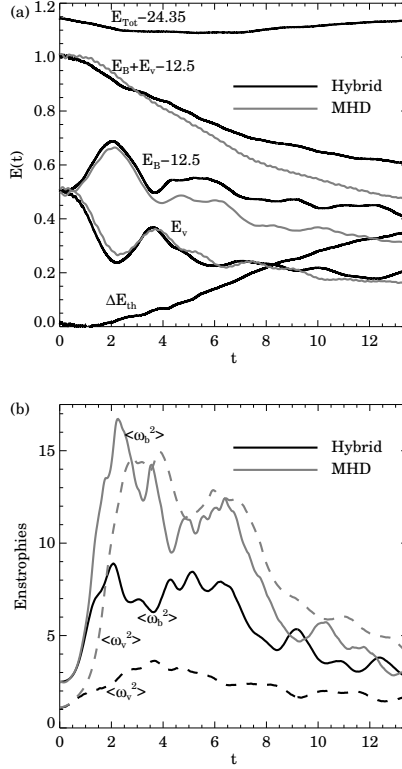


FIG. 2: Hybrid and MHD comparison: (a) Magnetic energy E_B , fluid flow energy E_v , their sum, the change in thermal energy ΔE_{th} , and total energy E_{Tot} vs. time. (b) Flow enstrophy $\langle \omega_v^2 \rangle$ and magnetic enstrophy $\langle \omega_B^2 \rangle$ vs. time.

enforces $\partial \nabla \cdot \mathbf{v} / \partial t = 0$ at $t = 0$. Simulations without the added perturbation show only small differences.

The hybrid simulation results are compared to results obtained using the compressible 2.5 D MHD code F3D [16] with constant and uniform resistivity $\eta = 0.0048$, zero viscosity ν , and ratio of specific heats $\gamma = 5/3$. (We motivate values for η and ν later.) In both cases, the magnetic islands initially centered on the midplane ($y = \pi$) begin to rotate in the clockwise direction. The initial velocity profile shears the magnetic islands until $t \sim 2$ as the islands approach and undergo a brief period of magnetic reconnection from $t \sim 2 - 4$. After $t \sim 4$, the system is dominated by self-similar turbulence. A comparison of out-of-plane current density J_z and magnetic field lines at $t = 1.96$ is shown in Fig. 1. The hybrid and MHD results show strong similarities at large scales, but significant differences at small scales where kinetic effects become important.

We can quantify the differences by comparing energy and dissipation budgets. Define

flow energy $E_v = \langle \rho |\mathbf{v}|^2 / 2 \rangle$, magnetic energy $E_B = \langle |\mathbf{B}|^2 / 2 \rangle$, thermal energy E_{th} (difference between total proton kinetic energy and proton flow energy), and total energy E_{tot} . The symbol $\langle \dots \rangle$ denotes a volume average. Grid scale fluctuations in the hybrid data are smoothed using a standard local, weighted iterative averaging.

Figure 2(a) shows E_v, E_B , their sum, ΔE_{th} (where Δ means the change since $t = 0$) and E_{tot} , as a function of time from the hybrid simulation (dark lines) and the MHD simulation (gray lines), with the magnetic energies shifted down by constants so that they appear on the same plot. Note that E_{tot} changes very little over the course of the hybrid run, demonstrating good numerical energy conservation. During the initial phase ($t < 2$), bulk flow energy is converted strongly into magnetic energy as field lines are stretched, but with little proton heating. The magnetic energy converts back to flow energy (with some heating) during the reconnection event ($t \sim 2 - 4$). Until $t \sim 4$, the energetics of the hybrid and MHD results are very similar. However, in the turbulent phase ($t > 4$), the hybrid and MHD codes show significant differences, and more dissipation occurs in the MHD case. Notably, the proton thermal energy increases monotonically during the turbulent phase in the hybrid simulation, even without explicit dissipation.

In MHD, the enstrophy is directly proportional to the rate of energy dissipation. Although the hybrid code lacks explicit dissipation, it is instructive to compare, see Fig. 2(b), the out-of-plane flow enstrophy (mean square vorticity) $\langle \omega_v^2 \rangle = \langle |\hat{\mathbf{z}} \cdot (\nabla \times \mathbf{v})|^2 \rangle$ and out-of-plane magnetic enstrophy (mean square current density) $\langle \omega_B^2 \rangle = \langle |\hat{\mathbf{z}} \cdot (\nabla \times \mathbf{B})|^2 \rangle = \langle J_z^2 \rangle$ in the hybrid (dark lines) and MHD (gray lines) simulations. At early time ($t < 4$), the hybrid magnetic and flow enstrophies peak at about same time as their MHD counterparts, but their magnitudes are very different, indicating that the length scales in the hybrid case are larger, which is probably due to finite larmor radius effects. During the turbulent phase ($t > 4$), the flow enstrophies continue to be different but the magnetic enstrophies are surprisingly similar. This suggests that the kinetic dissipation may resemble a classical resistivity, and we revisit this below. Note that the value of enstrophy in the hybrid case is necessarily sensitive to the averaging that defines the fluid scales.

To quantify the dissipation, consider the flow of magnetic energy in the system. Dotting the induction equation [Eq. (4)] with \mathbf{B} , averaging over space, and integrating over time

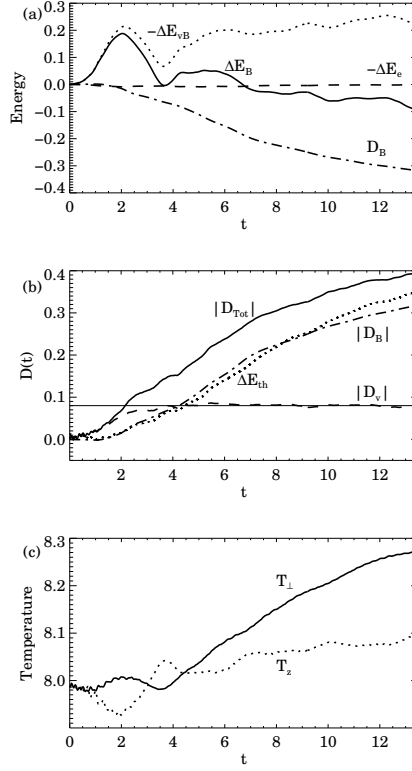


FIG. 3: (a) ΔE_B : change of E_B in the hybrid run; ΔE_{vb} : exchange between E_v and E_B ; ΔE_e : electron kinetic energy; \mathcal{D}_B : sum of these, total E_B dissipated. (b) \mathcal{D}_v and \mathcal{D}_B are cumulative dissipation through bulk flow and magnetic channels, \mathcal{D}_{tot} their sum, ΔE_{th} change in thermal energy. (c) Parallel and perpendicular proton temperatures vs. time.

gives

$$\Delta E_B(t) = - \int_0^t \langle \mathbf{v} \cdot (\mathbf{J} \times \mathbf{B}) \rangle dt' - \frac{d_e^2}{2} \langle \Delta J^2(t) \rangle - \mathcal{D}_B(t), \quad (5)$$

where Δ refers to the change since $t = 0$. The $\mathbf{v} \cdot (\mathbf{J} \times \mathbf{B})$ term exchanges energy between bulk flow and the magnetic field and the d_e^2 term is essentially the electron kinetic energy. We define \mathcal{D}_B as the cumulative energy dissipated from the magnetic channel. Included in this term are non-MHD dissipative processes and grid scale dissipation. The first three terms are calculable from the simulations, so we may compute \mathcal{D}_B .

Fig. 3(a) shows that for $t < 4$, E_B increases due to input from E_v , then decreases as it is converted back. In the turbulent phase ($t > 4$), there continues to be conversion into magnetic energy. However, E_B decreases during this period, and both energy converted from the flow, and an approximately equal amount previously stored in the field, is absorbed in

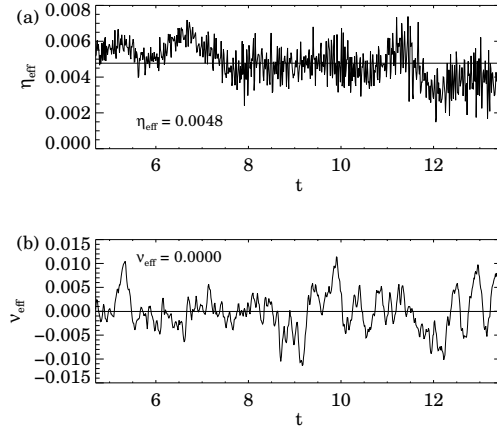


FIG. 4: Effective (a) resistivity η and (b) viscosity ν vs. time.

the magnetic dissipation \mathcal{D}_B .

A similar analysis can be done for energy flow in the bulk flow channel. Dotting the MHD momentum equation with \mathbf{v} and integrating over time and space gives

$$\Delta E_v(t) = \int_0^t \langle \mathbf{v} \cdot (\mathbf{J} \times \mathbf{B}) \rangle dt' - \mathcal{D}_v(t), \quad (6)$$

where \mathcal{D}_v is the cumulative energy converted into heat from the flow channel through non-fluid effects and compression. Fig. 3(b) shows D_v (dashed line), \mathcal{D}_B (dot-dashed), $\mathcal{D}_B + \mathcal{D}_v$ (solid), and ΔE_{th} (dotted). In the turbulent phase ($t > 4$), there is essentially no energy dissipated away through the flow channel (\mathcal{D}_v is flat). The energy dissipated through the magnetic field \mathcal{D}_B traces very closely the increase in thermal energy of the protons ΔE_{th} , so the main source of dissipation in this system is through magnetic interactions. The small departure between the two is accounted for by numerical heating, seen in the change in total energy E_{tot} [see Fig. 2(a)]; this is only about 10 % of the physical magnetic heating.

It appears reasonable that little dissipation occurs through the flow channel in a collisionless kinetic plasma. As energy cascades to smaller scales, the proton gyroradius is reached before the dissipation scale. Below the proton gyroradius, the ions decouple from the magnetic field and only weakly participate with the non-MHD waves in this region. Also the Alfvén ratio goes to zero in the kinetic regime as evidenced by the structure of kinetic Alfvén and whistler waves.

The increase in thermal energy of the protons due to dissipation from the magnetic field goes mainly into the temperature of the protons in the direction perpendicular to the guide

field, as shown in Fig. 3(c). The perpendicular and parallel temperatures T_{\perp} and T_{\parallel} are calculated from the pressure tensor divided by the density. In the turbulent phase ($t > 4$), T_{\perp} increases monotonically, while T_{\parallel} remains relatively steady. This is a central result of the present study: perpendicular heating of the protons occurs in the cascading Orszag-Tang system without any obvious connection to standard cyclotron resonances, as the latter generally are construed [11] to involve gyroresonance with parallel propagating waves, which are absent in the present 2.5 D system.

Finally, we investigate the nature of effective transport coefficients from the hybrid simulation. By assuming the classical functional forms for the dissipation $\eta \langle J_z^2 \rangle$ and $\nu \langle \omega_v^2 \rangle$, we can compute effective in-plane transport coefficients η_{eff} and ν_{eff} from the hybrid simulations. Figure 4 shows $\eta_{\text{eff}} = (\partial \mathcal{D}_b / \partial t) / \langle J_z^2 \rangle$ and $\nu_{\text{eff}} = (\partial \mathcal{D}_v / \partial t) / \langle \omega_v^2 \rangle$ as a function of time in (a) and (b), respectively. Surprisingly, the spatially averaged η_{eff} is fairly constant in time, as is often assumed in MHD models. The mean value is $\eta_{\text{eff}} = 0.0048$, corresponding to a Lundquist number of $S_{\text{eff}} = 4\pi V_0 L / \eta_{\text{eff}} c^2 \approx 1308$, equivalent to the magnetic Reynolds number for our system. In classical turbulence theory, the Reynolds number is related to the length scale at which dissipation occurs λ_d and energy containing scale L through $S_{\text{eff}} \sim (L/\lambda_d)^{4/3}$ [17]. Using S_{eff} , we can solve for λ_d for our system, giving $\lambda_d \sim 0.029$. This is of the order of the electron skin depth in our system, $c/\omega_{pe} \sim 0.049$. On the other hand, the spatially averaged ν_{eff} shows oscillations much larger than the mean, calling into question the assumption of a non-zero viscosity assumed in many MHD models.

That the effective resistivity is fairly constant does not necessarily imply that the dissipation is of the form ηJ^2 . In addition, the MHD simulations performed with this η_{eff} show more dissipation of B than the hybrid simulations, and cannot reproduce the preferential heating of T_{\perp} . We are currently investigating the spatial variations of these quantities to determine whether the in-plane dissipation is proportional to \mathbf{J} , as in MHD models. Another future study includes determining the dependence of η_{eff} on system size and/or proton and electron inertial scales. Finally, the physical mechanism which converts magnetic energy into proton heat remains an open question. Potential explanations are wave-particle interactions such as Landau damping. The details of this are under investigation.

This work is supported by NSF, NASA and NERSC.

-
- [1] S. R. Cranmer, Space Sci. Rev. **101** 229–294 (2002)
- [2] C. W. Smith et al., Astrophys. J. **645**, L85-L88, (2006)
- [3] D. Sundkvist et al., Phys. Rev. Lett., **99** 02004 (2007)
- [4] S. R. Spangler, Astrophys. J. **403**, 563 (2003)
- [5] L. Burlaga, *Interplanetary Magnetohydrodynamics* (OUP, New York, 1995).
- [6] C.-Y. Tu and E. Marsch, Space Sci. Rev. **73**, 1 (1995).
- [7] M. L. Goldstein et al., Annu. Rev. Astron. Astrophys. **33**, 283 (1995).
- [8] M. L. Goldstein et al., Springer Lecture series in Physics (1999).
- [9] S.A. Orszag and C.-M. Tang, J Fluid Mech. **90**, 129 (1979).
- [10] D. Rosenberg et al., New Journal of Physics **9**, 304 (2007).
- [11] P. A. Isenberg et al., J. Geophys. Res. **106**, 5649 (2001).
- [12] R. B. Dahlburg and J. M. Picone, Phys. Fluids B **1**, 2153 (1989).
- [13] A. Matthews et al., Lecture Notes in Physics **462**, (1995).
- [14] M. A. Shay et al., J. Geophys. Res. **106**, 3715 (2001).
- [15] U. Trottenberg et al., *Multigrid* (Academic Press, San Diego, 2000).
- [16] M. A. Shay et al., Phys. Plasmas **11**, 2199 (2004).
- [17] G. K. Batchelor, *The theory of homogeneous turbulence* (Cambridge University Press, Cambridge, 1953).